Investigation of the Elastoplastic and Viscoelastic Properties of Polyethylene through Cylindrical Indentation

LAURENTIU SANDU, CATALIN FETECAU*, FLORIN SUSAC, FELICIA STAN
Dunarea de Jos University of Galati, Faculty of Engineering,47 Domneasca, 800008, Galati, Romania

In this paper, the elasto-plastic and viscoelastic properties of two grades of polyethylene are investigated by cylindrical macro-indentation. Indentation tests, including relaxation tests, are performed with a cylindrical indenter having a flat-tip diameter of 1 mm. The bulk properties, such as the indentation modulus and the yield stress, are extracted from the indentation stress-displacement curves. The indentation relaxation data of polyethylene are analyzed using the steady-state creep model and the generalized Maxwell model. Based on experimental data and the Prony series model, equilibrium stress, relaxation ratio and relaxation time are determined, while the creep exponent and the characteristic relaxation time are estimated using the steady-state creep model.

Keywords:cylindrical macro-indentation, relaxation tests, steady-state creep model

The use of polymeric materials in engineering applications is growing more and more all over the world, from aerospace and automotive to electric and electronic industries. Since working conditions are different for each application, the knowledge of their mechanical behaviour, including viscoelastic behaviour, is particularly important in this context.

The determination of the local properties of polymeric materials, including in-service creep and relaxation behaviour, is required for structural design. The traditional material testing methods (tensile, compression, bending, etc.) are relatively simple and give different information on the behaviour of polymeric materials, but they are destructive, time and material consuming, and cannot be applied to extract local properties from final products. The final manufactured parts have dimensions that differ from those of the testing specimens and therefore the measurement of mechanical properties directly on the parts, at the end of the manufacturing process, is likely to provide improved understanding on the mechanical properties of the polymeric parts in correlation with the size scale and processing parameters [1-5].

The performances of semi-crystalline polymeric materials and consequently of the final products are related to many aspects, such as the final crystal structure (crystallization degree, size and distribution of the crystallites), residual stresses, molecular orientation, etc. [6, 7], which in turn are closely influenced by manufacturing techniques, such as injection molding, compression molding or extrusion [5-8]. For example, products which result from the injection molding process, due to high pressure, temperature and shear rates, develop a frozen skin on the outside walls (below the part surface) with a morphology that differs from that of the core of the part, i.e., the frozen layer is highly oriented in the frozen skin as compared with the core of the part with low molecular orientation [6-7].

In this paper, the advantages of the indentation technique became a useful tool for extracting local properties, macro-indentation with a cylindrical indenter being considered to extract the viscoplastic and time dependent properties of injection molding specimens. Indentation and stress relaxation tests are performed using a cylindrical indenter having a flat-tip diameter of 1 mm. The bulk properties are extracted from indentation stress-displacement curves, while the stress relaxation data are analyzed using two models: the steady-state creep model and the generalized Maxwell model. Uniaxial tensile tests are also carried out in order to correlate the indentation data to the tensile data.

Experimental part

Cylindrical indentation

The instrumented indentation method is based on the local deformation produced by an indenter upon application of a given load [9]. During an indentation test, the applied load on the indenter is continuously measured as a function of the indentation depth. Instrumented indentation is a widely-used technique to evaluate the elastic modulus, hardness, yield strength, and the strain hardening exponent from the load-displacement data [9-20]. For polymers, the main obstacle when using sharp indenters, such as pyramidal, conical or spherical indenters, is the determination of the true contact depth and the corresponding true contact area [9-14]. Depending on the type of the indented material, the true contact area is influenced by the pile-up and sink-in of the material, primarily affected by its plastic properties [9-14]. Therefore, the knowledge of the relationship between the indentation load and the true contact area is essential to extract the mechanical properties by indentation. In contrast, the contact area under a cylindrical indenter is constant and the deformation under the cylindrical indenter can quickly reach a steady plastic flow state [15-20]. Moreover, the cylindrical indentation methodology is much simpler compared with the commonly used spherical or sharp indentation [15-20].

As shown in figure 1, the loading indentation curve obtained by cylindrical indentation has two linear regions [20]: the first is dominated by elastic deformation, while

* *email: catalin.fetecau@ugal.ro*

the second, the so-called hardening region, is dominated by plastic deformation. Figure 1 shows that the load versus indentation displacement curve has a characteristic point, Y, which defines the transition from the elastic to the plastic region. Based on the load-displacement curve, three parameters can be directly obtained [20]:

(i) the indentation modulus, *IM*, defined as the slope of the stress-displacement curve in the elastic region;

(ii) the critical transition force, *CTF*, or the load level where the material loses its linear behaviour;

(iii) the mean indentation pressure or hardness, *H*, defined as:

$$H = \frac{F_Y}{A_{tip}} \quad (1)$$

where $A_{tip} = \pi R^2$ represents the contact area of the flat-tip indenter and F_y is obtained by extrapolating the linear part of the hardening curve back to the vertical axis and measuring the interception with this axis (fig. 1).

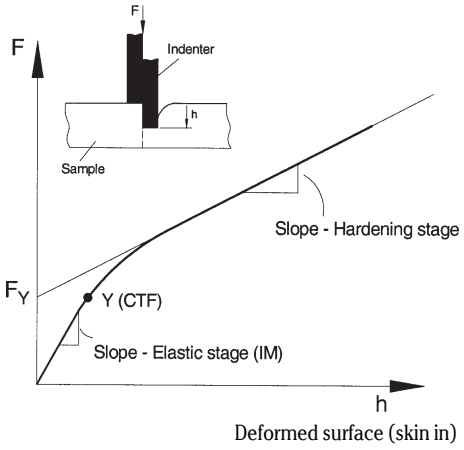

Fig. 1. Load-displacement curve for cylindrical indentation

The material yield stress can be related to the hardness through the following relation [17, 21, 22]

$$\sigma_Y = \frac{H}{C} \quad (2)$$

where *C* is a constant which depends on the indented material.

For indentation relaxation, a two-step indentation test is carried out [20]: loading – the sample is subject to loading up to a constant indentation depth, h_0, and holding – the displacement is kept constant and the relaxation is measured as a function of time, as shown in figure 2. Depending on the controlled variable in the loading step, the indentation test can be carried out using two approaches: the displacement-controlled test if the indentation depth is controlled, and the load-controlled test if the controlled variable is the load.

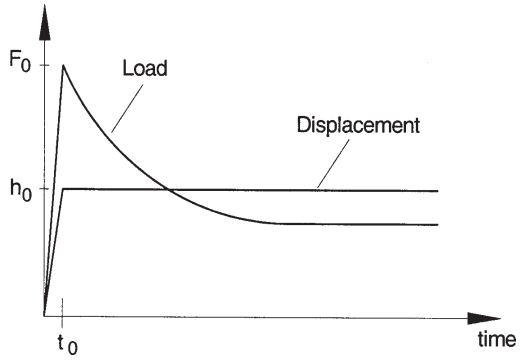

Fig. 2. Indentation relaxation test - applied displacement and corresponding load history

To determine the viscoelastic material function during the indentation relaxation test, the generalized Maxwell model is considered [23]. In this model, the time-dependent stress is represented by the Prony series [20, 23]

$$\sigma(t) = \sigma_\infty + \sum_{k=1}^{N} \sigma_k \exp\left(-\frac{t}{\tau_k}\right) \quad (3)$$

where σ_∞ is the equilibrium stress, $\tau_k = \eta_k / \sigma_k$ is relaxation time of the *k*-th Maxwell element, σ_k is the Prony coefficient of the *k*-th Maxwell element, and *t* is time.

For a linearly elastic material, the relaxation function can be calculated by [20, 23]

$$E(t) = \frac{\sigma(t)}{\varepsilon_0} = E_\infty + \sum_{k=1}^{N} E_k \exp\left(-\frac{t}{\tau_k}\right) \quad (4)$$

where ε_0 is the initial applied strain, E_∞ is the long-term modulus (equilibrium modulus), and E_k is the Prony coefficient of the *k*-th Maxwell element.

The instantaneous modulus E_0 or the glassy modulus (equivalent to Young's modulus), which characterizes the mechanical behaviour of viscoelastic materials in the shorter relaxation time regime, is given by [23]

$$E_0 = E_\infty + \sum_{k=1}^{N} E_k . \quad (5)$$

Viscoelastic behaviour is linear when the value of $E(t)$ is independent of the initial strain ε_0 [23].

Since creep and stress relaxations are both aspects of the time-dependent behaviour, another approach to determine the stress relaxation function is to consider the inter-conversion relation and the steady-state creep model [20, 24, 25].

After the beginning of the indentation relaxation stage, the initial total strain, ε_0, is constant and represents the superposition of the reversible elastic strain and the irreversible inelastic strain, $\varepsilon_0 = \varepsilon_e + \varepsilon_{in}$. The inelastic strain is the sum of the plastic strain and the creep strain, $\varepsilon_{in} = \varepsilon_p + \varepsilon_{cr}$. During the relaxation stage, the plastic strain is irreversible and equals to its initial value; therefore $d\dot{\varepsilon}_p = 0$.

If the creep strain is defined in terms of the power-law model [25],

$$d\dot{\varepsilon}_{cr} = A\dot{\varepsilon}^m , \quad (6)$$

then the behaviour of a viscoelastic material during the stress relaxation can be described by the following equation [20, 24-26]

$$\sigma(t) = \left\{\sigma_0^{(1-m)}\left[1 + (m-1)\frac{t}{\lambda}\right]\right\}^{1/(1-m)} \quad (7)$$

where σ_o is the initial stress, *t* is time, *m* and λ are the steady-state creep rate exponent and the characteristic relaxation time of the material constant, respectively.

Materials and experiments

The polymers used in this study are a commercial injection molding High-density Polyethylene (HDPE, J2200 supplied by Russia) and a Low-density Polyethylene (LDPE, ROPOTEN, supplied by Bulgaria).

Dog-bone specimens were prepared by injection molding using an Arburg injection molding machine (Arburg Allrounder 320 C 500–170, Germany). The injection molding parameters are presented in table 1. The samples have a cross-section area of 10×4 mm^2 and a straight central length of 60 mm, as shown in figure 3a.

The indentation tests were carried out on a Testometric universal testing machine (Model M350 – 5AT, UK) with a 5kN load cell. Two crosshead speeds were considered, such as 1 and 5 mm/min. All indentation tests were performed at room temperature (23°C) with a cylindrical

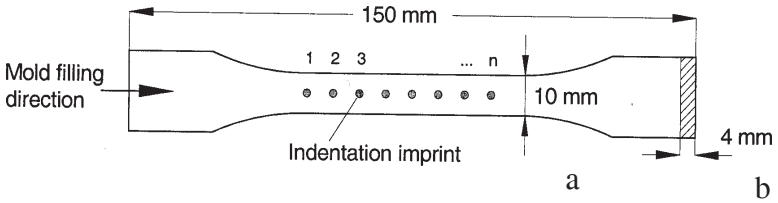

Fig. 3. Geometry of the injection molding specimen (a) and cylindrical indentation set-up (b)

Table 1
PROCESSING PARAMETERS IN THE INJECTION MOLDING PROCESS

Parameter	LDPE	HDPE
Melt temperature (°C)	220	255
Mold temperature (°C)	30	30
Flow rate (cm^3/s)	7	17
Holding pressure (MPa)	65	100
Cooling time (s)	12	13

flat indenter made of tungsten carbide, having a tip diameter of 1 mm and an active length of 2 mm (fig. 3b).

The indentation tests were performed along the mold filling direction to investigate the variation of the mechanical performances and anisotropy along the specimen (fig. 3a). The indentation tests were run to an indentation depth of at least one diameter, and the distance between two indentation imprints was five diameters. At least five specimens were tested for each crosshead speed. For each specimen, the indentation modulus, the critical transition load and the yield stress were extracted.

The indentation relaxation tests were carried out at room temperature using the same cylindrical indenter. The indentation relaxation response was measured using a load-controlled procedure: firstly, the samples were loaded to an initial indentation load, F_0, which corresponds to an initial displacement, h_0, then the crosshead was stopped and the decrease of the load as a function of time was continuously recorded. The length of the relaxation tests was set to 300 s.

Also the tensile tests were also carried out in order to correlate the indentation results with the results obtained from the tensile testing method. The tests were conducted on the same dog-bone specimens with a crosshead speed of 1 and 5 mm/min, corresponding to a constant initial strain rate of 1.45×10^{-4} and 7.25×10^{-4} s^{-1}, respectively, for the applied clamp-to-clamp distance of 115 mm.

Results and discussions

Indentation load-displacement results

Figure 4 shows the indentation curves on HDPE and LDPE at a crosshead speed of 1 mm/min. Since the contact area remains constant during indentation with a cylindrical flat-tip indenter, the indentation stress was defined as the ratio between the applied load and the cross-section area. The indentation strain under the indenter was taken as the indentation displacement normalized with respect to the diameter of the indenter [17, 18, 20].

As shown in figure 4, the indentation curves have an initial linear stage with a strong elastic contribution followed by a curved part and, finally, at high penetration depths, by

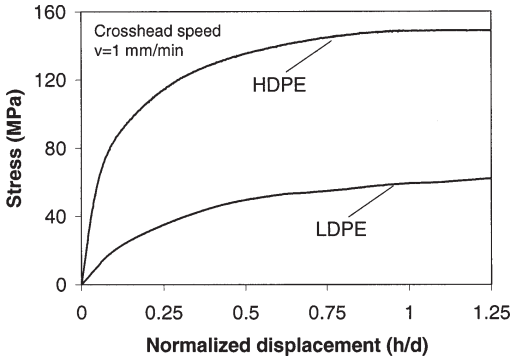

Fig. 4. Indentation stress-displacement curves for polyethylene

an almost linear deformation stage with a strong hardening contribution.

The indentation tests carried out at least six times on each specimen generated similar load-displacement curves, but not identical, especially in the hardening region. For HDPE, the indentation stress reaches a plateau at indentation depths greater than about 0.75 mm. Almost no changes in the indentation load were recorded with further increase in the indentation depth. For LDPE, the indentation stress increases with increasing indentation depth and has a finite slope.

The indentation modulus was determined as the slope of the stress-normalized displacement curve in the elastic stage, as shown in figure 1. The slope variation in the elastic region is presented in figure 5. The results appear relatively scattered in the longitudinal direction of the specimens, especially for HDPE (fig. 5a). The elastic modulus slightly decreases with increasing distance from the injection gate. This could be explained by the fact that the polymer flow inside the specimen during injection molding results in variation of morphology.

During the indentation tests, the steady-state condition of constant plastic zone size should be reached in order to relate the stress-displacement curve to the yield stress. It is generally accepted that steady-state conditions are reached for an indentation displacement exceeding one diameter [14-20]. From the stress distribution under the indentation, a linear dependence of the indentation stress on normalized displacement was observed starting from a displacement greater than 0.75 mm. It should be noted that the maximum indentation depth was 1.25 mm, limited by the thickness of the specimen. The linear portion of the stress-displacement curve was extrapolated back to the vertical axis in order to calculate the mean indentation pressure, as shown in eq. (1) and figure 1. The properties

Parameters	HDPE	LDPE
Indentation tests		
Indentation modulus, *IM* (MPa)	970 ± 97.5	150 ± 2.5
Critical transition force, CTF (N)	39 ± 2.5	15 ± 0.15
Mean indentation pressure, p_m (MPa)	145 ± 0.6	48 ± 1.5
Tensile tests		
Tensile Young's modulus, *E* (MPa)	960 ± 47.6	155 ± 3
Tensile yield stress, σ_Y (MPa)	18 ± 0.3	7.5 ± 0.05

Table 2
PROPERTIES OF HDPE AND LDPE, v=1 mm/min

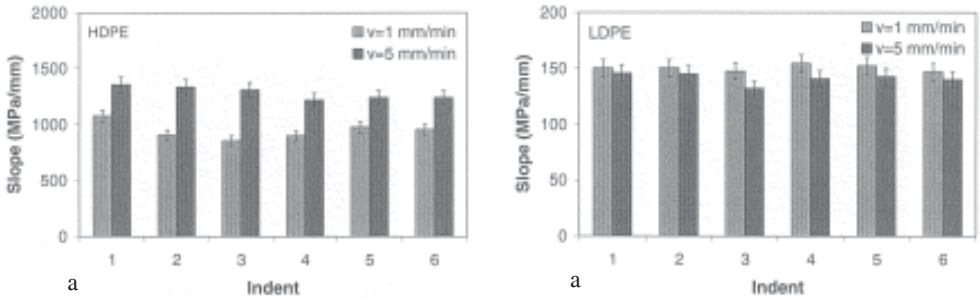

Fig. 5. Slope of the stress-normalized displacement curves in the elastic stage for HDPE (a) and LDPE (b)

extracted from the stress-displacement indentation curves for 1 mm/min are given in table 2. These values represent the average along the molding direction for five specimens. The standard deviation is also given in table 2.

Young's modulus and yield stress were also determined from tensile tests using injection molded specimens. The representative true stress-strain curves are plotted in figure 6. Young's modulus was defined as the slope of the initial linear zone of the true stress-strain curve. The yield point (the onset of plastic deformation) was defined as the point where the stress-strain curve shows a local maximum. It should be noted that this definition is generally accepted for polymers.

As shown in figure 6, for LDPE, during the tensile tests, no stress drop is observed after yielding, and strain hardening takes place at higher strains. For HDPE, there is a stress drop after yielding followed by necking initiation and propagation along the specimen. The results and the fact that the tensile Young's modulus is in good agreement with the value extracted from the indentation tests are also presented in table 2.

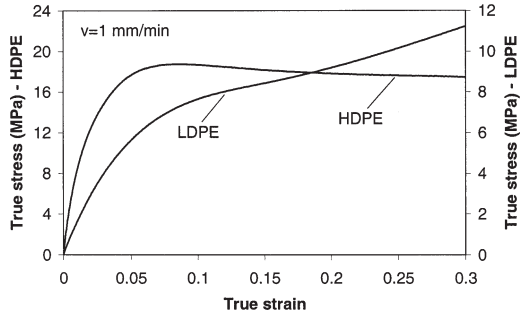

Fig. 6. Tensile true stress-strain curves at 1 mm/min crosshead speed

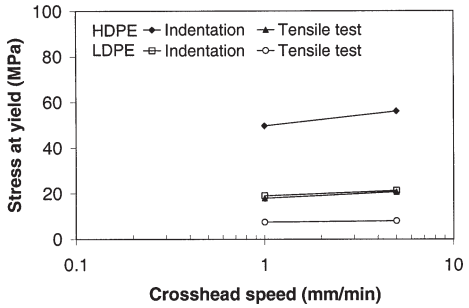

Fig. 7. Comparison between indentation and tensile yield stress

One of the issues in the present study is the correlation between the mean indentation pressure and the tensile yield stress. Several studies have suggested that the ratio between the mean indentation pressure and the yield stress is less than 3 [16, 17, 21]. However, we have found that, for indentation on polyethylene, this ratio is higher than 3.

In order to derive the correlation between the indentation and the tensile results, the mean indentation pressure was calculated based on the critical transition force (CTF) which corresponds to the yield point at which the material

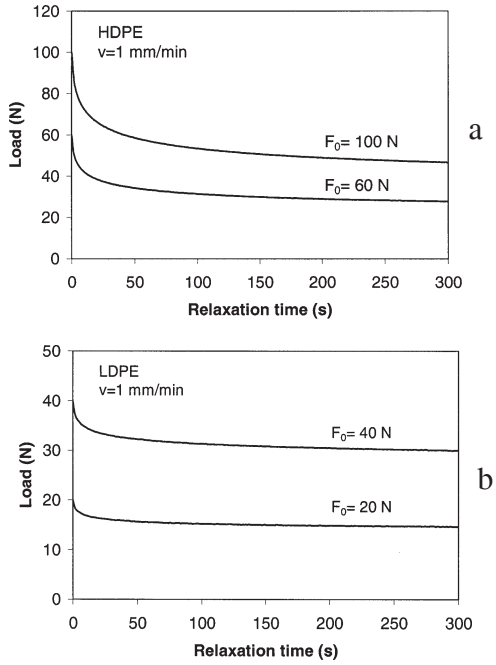

Fig. 8. Indentation relaxation curves for HDPE (a) and LDPE (b)

begins to deform plastically. Figure 7 presents the tensile yield stress and the indentation yield stress (calculated based on the CTF) as a function of the crosshead speed. In this case, the ratio between the tensile yield stress and the indentation yield stress calculated based on the critical transition force is 2.5 for LDPE and 2.75 for HDPE.

Indentation relaxation results

Figure 8 shows the variation of the indentation relaxation load with time for two initial relaxation loads. For HDPE, the initial relaxation load was set to 60 N and 100 N, respectively, while for LDPE, the initial relaxation load was set to 20 N and 40 N, respectively.

The load drops steeply at the beginning of the relaxation process and then monotonically decreases with time, approaching a relaxation limit depending on the applied strain/stress level, as shown in figure 8.

The stress relaxation data were directly fitted to eq. (3). The corresponding material parameters were determined from the minimization of the following function [20]

$$\sum_{k=1}^{N}\left(\frac{\sigma_k^{exp}-\sigma_k^{mod}}{\sigma_k^{exp}}\right)^2 \quad (8)$$

where σ_{exp} is a point on the experimental curve and σ_{mod} is a point calculated using eq. (3).

For the fitting procedure, the values of the relaxation time were fixed along the logarithmic time scale [20, 27]. A Maxwell model controls the (linear) viscoelastic behaviour over roughly 1.5 logarithmic decades [28]. Since, the experimental data cover about 2.5 decades, three terms in the Prony series were sufficient to accurately fit the experimental data. The model parameters are

Table 3
PRONY SERIES CONSTANTS FOR LDPE

	v= 1 mm/min		v= 5 mm/min		
	F_0=20 N	F_0=40 N	F_0=20 N	F_0=40 N	
τ (s)	18.665	38.120	16.358	34.451	σ_∞
1	2.045	3.571	4.732	7.500	σ_1
10	2.646	4.423	2.720	4.866	σ_2
100	2.140	4.879	1.742	4.129	σ_3

Table 4
PRONY SERIES CONSTANTS FOR HDPE

	v= 1 mm/min		v= 5 mm/min		
	F_0=60 N	F_0=100 N	F_0=60 N	F_0=100 N	
τ (s)	58.504	34.809	30.458	50.333	σ_∞
1	15.067	11.294	19.085	30.500	σ_1
10	27.412	16.243	14.758	26.157	σ_2
100	26.386	14.209	12.265	20.254	σ_3

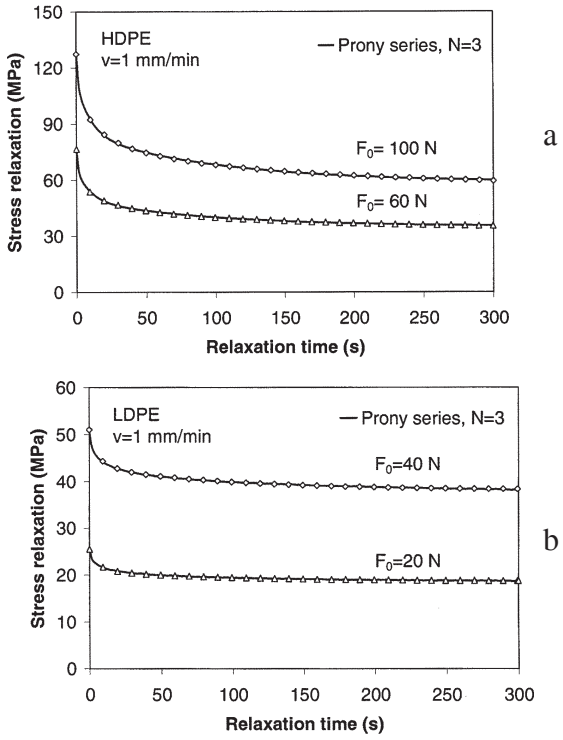

Fig. 9. Comparison between experimental data and Prony series model for indentation relaxation on polyethylene (open symbols denote the experimental data)

presented in tables 3 and 4, while the comparison between the experimental data and the Prony series model is shown in figure 9. The Prony series model provides a very good description of the experimentally measured stress relaxation data, as shown in figure 9 (coefficient of determination, R^2=0.999). In order to obtain the relaxation function in terms of Young's moduli, the coefficients presented in tables 3 and 4 must be simply divided by the initial strain, as shown in eq. (4).

Regarding the behaviour of polyethylene during the indentation relaxation tests, three stages were identified, as shown in figure 9 and tables 3 and 4: a very fast decreasing stress relaxation due to the lack of movement between chains, a slowly decreasing stress with possible macromolecular chains mobility and reorientation of chains under applied loads, and a constant stress characterizing an equilibrium response, σ_∞.

The stress relaxation data were also fitted to eq. (7). The least-squares fitting was carried out to determine a set of best-fit parameters based on minimizing the following error function [20]

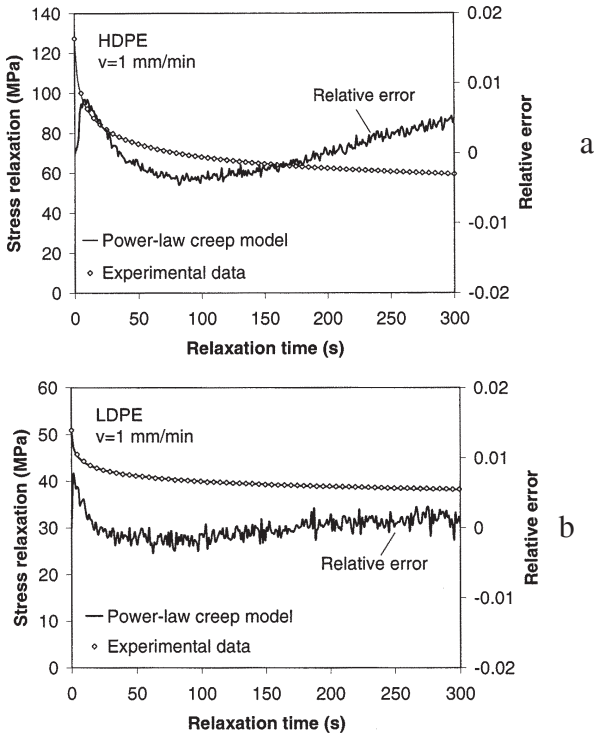

Fig. 10. Comparison between experimental data and power-law creep model for indentation relaxation on polyethylene with 1 mm cylindrical flat-tip indenter

Table 5
STEADY-STATE CREEP MODEL PARAMETERS, v=1 mm/min

Material	F_0 (N)	λ (s)	m	RMSE
HDPE	60	4.50	9.05	2.0×10^{-1}
	100	6.93	8.53	2.2×10^{-1}
LDPE	20	3.68	25.27	8.6×10^{-2}
	40	7.56	24.70	6.8×10^{-2}

Table 6
STEADY-STATE CREEP MODEL PARAMETERS, v=5 mm/min

Material	F_0 (N)	λ (s)	m	RMSE
HDPE	60	1.47	9.08	2.0×10^{-1}
	100	1.55	8.92	4.4×10^{-1}
LDPE	20	0.17	24.61	1.3×10^{-1}
	40	0.70	24.43	1.5×10^{-1}

$$\sum_{k=1}^{N}\left(\sigma_k^{mod}-\sigma_k^{exp}\right)^2 \quad (9)$$

where σ_{exp} is a point on the experimental curve and σ_{mod} is a point generated from eq. (7).

The model parameters are presented in tables 5 and 6, while the stress relaxation curves corresponding to the steady-state creep model are presented in figure 10. The relative error, $(\sigma_{exp}-\sigma_{mod})/\sigma_{exp}$, between the experimental and the predicted stress is also plotted in figure 10. As shown in this figure, the stress predicted by the power-law creep model fits very well the experimental data, with a maximum relative error less than 0.1%. The performance of the fitting procedure was also assessed using the root mean squared error (RMSE), as shown in tables 5 and 6.

Based on the power-law creep model, it was found that the creep exponent for the HDPE is lower than that for LDPE. The crosshead speed and the initial load have very little influence on the creep exponent. The increase of the crosshead speed decreases the characteristic time, while the increase of the initial load slightly increases the characteristic time. Regardless of the initial load and the crosshead speed values, during the characteristic

relaxation time the stress drops off drastically, nearly 87% of its initial value for the LDPE, and nearly 76% of its initial value for the HDPE.

Conclusions

In this paper, indentation tests have been performed with a cylindrical flat-tip indenter of 1 mm in diameter in order to extract the viscoplastic and time-dependent properties, such as stress relaxation, of injection molded polyethylene specimens. Based on the experimental load-displacement curves, the indentation modulus, the critical transition load and the indentation mean pressure were determined.

A good agreement was found between the mean value for the indentation modulus calculated from the indentation tests and Young's modulus obtained from the tensile tests. Also, it was found that the ratio between the tensile yield stress and the indentation yield stress calculated based on the critical transition load is about 2.5 for LDPE and 2.75 for HDPE.

The stress relaxation data were fitted to the steady-state creep model and the generalized Maxwell model. Both models fitted very well to the experimental data. Based on the steady-state creep model, it was found that the stress drops off during the characteristic relaxation time nearly 87 and 76% of its initial value for LDPE and HDPE, respectively.

This work confirms that, if dealing with the manufacturing of plastics, the cylindrical indentation method is an effective technique that can be used to evaluate the mechanical and viscoelastic properties of the parts in a non-destructive way.

Acknowledgements: This work was supported by the POS CCE Project P0102421/5117/22.05.2014 (COD SIM 50414).

References

1.SOUSA, R.A., REIS, R.L., CUNHA, A.M., BEVIS, M.J., Journal of Applied Polymer Science, **89**, 2003, p. 2079.
2.ZHANG, J., SHEN K., GAO Y., YUAN Y., Journal of Applied Polymer Science, **96**, 2005, p. 818.
3.ELLEUCH, R., TAKTAK, W., Journal of Materials Engineering and Performance, **15**, 2006, p. 111.
3. DUSUNCELI, N., COLAK, O.U., Materials and Design, **29**, 2008, p. 1117.5.
5.SANDU, L., STAN, F., FETECAU, C., ASME 2013 International Manufacturing Science and Engineering Conference, **1**, 2013, V001T01A065.
6.WANG, K., CHEN, F., ZHANG, Q., FU, Q., Polymer, **49 (22)**, 2008, p. 4745.
7.SCHRAUWEN, B.A.G., v. BREEMEN, L.C.A., SPOELSTRA, A.B., GOVAERT, L.E., PETERS, G.W.M., MEIJER, H.E.H., Macromolecules, **37**, 2004, p. 8618.
8.POSTOLACHE, I., FETECAU, C., STAN, F., NEDELCU, D., Mat. Plast., **47**, no. 4, 2009, p. 458.
9.CRIPPS FISCHER, A.C., Nanoindentation, 2nd Ed., Springer, 2004.
10.VRIEND, N.M., KREN, A.P., Polymer Testing, **23**, 2004, pp. 369.
11.BENABDALLAH, H. S., BUI, V. T., Polymer Engineering and Science, **44**, 2004, p. 1439.
12.SELTZER, R., MAI, Y.W., Engineering Fracture Mechanics, **75**, 2008, p. 4852.
13.KERMOUCHE, G., LOUBET, J.L., BERGHEAU, J.M., Mechanics of Materials, **40**, 2008, p. 271.
14.STAN, F., MUNTEANU, A.V., FETECAU, C, Mat. Plast., **48,** no. 1, 2011, p. 1.
15.BUCAILLE, J.L., FELDER, E., Journal of Materials Science, 37, 2002, pp. 3999.
16.RICCARDI, B., MONTANARI, R., Materials Science and Engineering A, **381**, 2004, p. 281.
17.LU, Y.C., SHINOZAKI, D.M., Journal of Engineering Materials and Technology, **130 (4)**, 2008, pp. 041001.
18.GUGLIELMOTTI, A., QUADRINI, F., SQUEO, A.E., Polymer Engineering and Science, **48**, 2008, p. 1279.
19.CAO, Y., MA, D., RAABE, D., Acta Biomaterialia, **5**, 2009, p. 240.
20.STAN, F., FETECAU, C., Composites Part B, **47**, 2013, p. 298.
21.TABOR, D., The Hardness of Metals, Clarendon Press, Oxford, 1951.
22.JOHNSON, L.L., Contact Mechanics, Cambridge University Press, Cambridge, 1994.
23.FERRY, J.D., Viscoelastic Properties of Polymers, 3rd Edn., Wiley, New York, 1980.
24.FERNANDEZ, P., RODRIGUEZ, D., LAMELA, M.J., FERNANDEZ-CANTELI, A., Mechanics of Time-Dependent Materials Journal, **15**, 2011, p. 169.
25.J. BETTEN, Creep Mechanics, 3rd Ed., Springer, 2008.
26.XU, Z., HOU, J, Mechanics of Time-Dependent Materials Journal, **15**, 2011, p. 29.
27.KNAUSS, W.G., ZHAO, J, Mechanics of Time-Dependent Materials, **11**, 2007, p. 199.
28.TSCHOEGL NW., Time Dependence in Material Properties: An Overview. Mechanics of Time-Dependent Materials, **1**, 1997, p. 3

Manuscript received: 4.05.2015